MIT Libraries | DSpace@MIT

MIT Open Access Articles

An Experimental and Analytical Study of the Evolution of Crystallographic Texturing in FCC Materials

Massachusetts Institute of Technology

AN EXPERIMENTAL AND ANALYTICAL STUDY OF THE EVOLUTION OF CRYSTALLOGRAPHIC TEXTURING IN FCC MATERIALS.

C. A. BRONKHORST, S. R. KALIDINDI, and L. ANAND

Department of Mechanical Engineering
Massachusetts Institute of Technology
Cambridge, Massachusetts 02139.

ABSTRACT

A Taylor type polcrystalline model, together with a new fully implicit time integration scheme have been developed to simulate the evolution of crystallographic texture during the deformation of face centered cubic metals deforming by crystallographic slip. The constitutive equations include a new equation for the evolution of slip system deformation resistance which leads to realistic macroscopic strain hardening behavior. The good predictive capabilities of the constitutive equations and the time integration procedure are demonstrated by comparing numerical simulations against experimental texture measurements and stress-strain results in a series of homogeneous deformation experiments on OFHC copper.

NOMENCLATURE

For the most part, we shall use direct tensor notation which is standard in modern continuum mechanics. Bold lower case symbols represent vectors, bold upper case symbols second order tensors, and bold calligraphic symbols fourth order tensors. No summation is implied on repeated indices. Tensor and vector arguments are omitted for brevity and whenever there is no danger of confusion. Also, '⊗' denotes a tensor product, while '·' denotes a scalar dot product.

INTRODUCTION

Asaro and Needleman[1] have developed an elastic-plastic, rate-dependent polycrystalline model for low homologous temperatures in which deformation within the individual crystals is taken to be by crystallographic slip alone. To predict the global response of the polycrystal, Asaro and Needleman follow the pioneering work of Taylor[2] and assume that all grains have equal volume, and that the deformation gradient within each grain has a uniform value throughout the aggregate.

The purpose of this paper is to give a brief report of (a) our new *fully-implicit* time-integration procedure for a slightly modified form of the polycrystalline constitutive model of Asaro and Needleman[1], and (b) a comparison of the results from our simulation procedures against the experimental results from uniaxial compression, uniaxial tension, plane strain compression, and simple shear on polycrystalline OFHC copper.

CONSTITUTIVE MODEL

With $\mathbf{T}^{(k)}$ denoting the Cauchy stress in the kth crystal, Taylor's assumptions lead to:

$$\bar{\mathbf{T}} = \frac{1}{N} \sum_{k=1}^{N} \mathbf{T}^{(k)}, \tag{1}$$

where $\bar{\mathbf{T}}$ is the volume averaged stress, and N is the total number of grains.

The equations for the stress in a grain is taken as

$$\mathbf{T}^* = \mathcal{L}\left[\mathbf{E}^*\right], \tag{2}$$

$$\mathbf{E}^* \equiv (1/2)\left\{\mathbf{F}^{*T}\,\mathbf{F}^* - \mathbf{1}\right\}, \tag{3}$$

$$\mathcal{L} \equiv 2\mu\mathcal{I} + (\kappa - (2/3)\mu)\,\mathbf{1} \otimes \mathbf{1}, \tag{4}$$

with $\mathcal{L}$ being the fourth order isotropic[1] elasticity tensor, μ and κ are the elastic shear and bulk moduli respectively, $\mathcal{I}$ and $\mathbf{1}$ the fourth and second order symmetric identity tensors respectively, and

$$\mathbf{T}^* \equiv \mathbf{F}^{*-1}\left\{(\det\mathbf{F}^*)\,\mathbf{T}\right\}\mathbf{F}^{*-T} \tag{5}$$

is the stress measure which is work conjugate to the elastic strain measure $\mathbf{E}^*$. Also, $\mathbf{T}$ is the symmetric Cauchy stress tensor in the grain, and $\mathbf{F}^*$ is a local elastic deformation gradient defined in terms of the local deformation gradient $\mathbf{F}$ (equal to the macroscopic $\mathbf{F}$) and a local plastic deformation gradient $\mathbf{F}^p$ by

$$\mathbf{F}^* \equiv \mathbf{F}\mathbf{F}^{p-1}, \qquad \det\mathbf{F}^* > 0, \qquad \det\mathbf{F}^p = 1. \tag{6}$$

The plastic deformation gradient is in turn given by the flow rule

$$\dot{\mathbf{F}}^p = \mathbf{L}^p\,\mathbf{F}^p, \tag{7}$$

$$\mathbf{L}^p = \sum_{\alpha}\dot{\gamma}^{\alpha}\,\mathbf{S}_0^{\alpha}, \qquad \mathbf{S}_0^{\alpha} \equiv \mathbf{m}_o^{\alpha} \otimes \mathbf{n}_o^{\alpha}, \tag{8}$$

where $\mathbf{m}_o^{\alpha}$ and $\mathbf{n}_o^{\alpha}$ are time independent, orthonormal unit vectors which define the slip direction and slip plane normal of slip system α in a fixed reference configuration, and $\dot{\gamma}^{\alpha}$ is the plastic shearing rate on this slip system. For an fcc crystal there are twelve $\{111\}<110>$ type slip systems.

The local configuration for a grain defined by $\mathbf{F}^p$ is an isoclinic relaxed configuration, and a plastic stress power per unit volume in this configuration may be defined[3] by

$$\dot{\omega}^p \equiv \mathbf{C}^*\mathbf{T}^* \cdot \mathbf{L}^p, \qquad \text{with} \quad \mathbf{C}^* \equiv \mathbf{F}^{*T}\mathbf{F}^*. \tag{9}$$

Using equations 8 and 9 we define a resolved shear stress τ^{α} for slip system α through the relation

$$\dot{\omega}^p = \sum_{\alpha}\tau^{\alpha}\dot{\gamma}^{\alpha}, \tag{10}$$

---

[1]In our simple model we neglect the elastic anisotropy of the single crystal.

which gives, $\tau^{\alpha} \equiv \mathbf{C}^* \mathbf{T}^* \cdot \mathbf{S}_0^{\alpha}$. For small elastic stretches we assume

$$\tau^{\alpha} \approx \mathbf{T}^* \cdot \mathbf{S}_0^{\alpha}. \tag{11}$$

Next, the plastic shearing rate on the slip system α is defined by

$$\dot{\gamma}^{\alpha} = \dot{\gamma}_o \left| \frac{\tau^{\alpha}}{s^{\alpha}} \right|^{1/m} \operatorname{sign}(\tau^{\alpha}), \tag{12}$$

where $\dot{\gamma}_o$ is a reference shearing rate, m is a strain rate sensitivity parameter, and s^{α} is the slip resistance on the slip system α.

Finally, the slip resistance s^{α} is taken to evolve as

$$\dot{s}^{\alpha} = \sum_{\beta} h^{\alpha\beta} \left| \dot{\gamma}^{\beta} \right|, \tag{13}$$

with $\qquad\qquad h^{\alpha\beta} = q^{\alpha\beta} h^{(\beta)} \qquad \text{(no sum on } \beta\text{)}, \tag{14}$

where $h^{(\beta)}$ is a single slip hardening rate, and $q^{\alpha\beta}$ is the matrix describing the latent hardening behavior of a crystallite[1].

TIME INTEGRATION PROCEDURE

Let τ denote a time Δt later than time t. Recall that the slip system $(\mathbf{m}_o^{\alpha}, \mathbf{n}_o^{\alpha})$ are time independent quantities; assume that these are known. Then given $\mathbf{F}(t)$, $\mathbf{F}(\tau)$ and the list $\{\mathbf{F}^p(t), s^{\alpha}(t), \mathbf{T}(t)\}$ in each grain, the time integration problem is to calculate $\{\mathbf{F}^p(\tau), s^{\alpha}(\tau), \mathbf{T}(\tau)\}$ in each grain, calculate the volume averaged stress $\bar{\mathbf{T}}(\tau)$ using equation 1, calculate the texture at time τ from

$$\mathbf{m}_{\tau}^{\alpha} = \mathbf{F}^*(\tau)\mathbf{m}_o^{\alpha} \implies \mathbf{m}_{\tau}^{\alpha} \approx \mathbf{R}^*(\tau)\mathbf{m}_o^{\alpha}, \tag{15}$$

$$\mathbf{n}_{\tau}^{\alpha} = \mathbf{F}^{*-T}(\tau)\mathbf{n}_o^{\alpha} \implies \mathbf{n}_{\tau}^{\alpha} \approx \mathbf{R}^*(\tau)\mathbf{n}_o^{\alpha}, \tag{16}$$

where $(\mathbf{m}_{\tau}^{\alpha}, \mathbf{n}_{\tau}^{\alpha})$ represents slip system α in the deformed configuration at time τ, and $\mathbf{R}^*(\tau)$ is the rotation in the polar decomposition

$$\mathbf{F}^*(\tau) = \mathbf{R}^*(\tau)\mathbf{U}^*(\tau), \quad \text{with} \quad \mathbf{F}^*(\tau) = \mathbf{F}(\tau)\mathbf{F}^p(\tau)^{-1}, \tag{17}$$

and march forward in time.

Using the constitutive equations, an Euler Backward time integration procedure, and the approximation

$$\mathbf{F}^p(\tau) \doteq \left\{ 1 + \sum_{\alpha} \Delta\gamma^{\alpha}\mathbf{S}_0^{\alpha} \right\} \mathbf{F}^p(t), \quad \text{with} \quad \Delta\gamma^{\alpha} \equiv \dot{\gamma}^{\alpha}(\tau)\,\Delta t, \tag{18}$$

for the integration of $\dot{\mathbf{F}}^p$, we obtain

$$\mathbf{T}^*(\tau) = \mathbf{T}^{*tr} - \sum_{\alpha} \Delta\gamma^{\alpha}\mathbf{C}^{\alpha}, \tag{19}$$

$$s^{\alpha}(\tau) = s^{\alpha}(t) + \sum_{\beta} h^{\alpha\beta}(\tau) \left| \Delta\gamma^{\beta} \right|, \tag{20}$$

where
$$\mathbf{T}^{*tr} \equiv \mu\,\mathbf{A} + \frac{3k-2\mu}{6}\,(\mathrm{tr}\mathbf{A})\mathbf{1} - \frac{3}{2}k\mathbf{1}, \tag{21}$$

$$\mathbf{A} \equiv \mathbf{F}^{p^{-T}}(t)\,\mathbf{F}^T(\tau)\,\mathbf{F}(\tau)\,\mathbf{F}^{p^{-1}}(t), \tag{22}$$

$$\mathbf{C}^\alpha \equiv \mu\,\mathbf{B}^\alpha + \frac{3k-2\mu}{6}\,(\mathrm{tr}\mathbf{B}^\alpha)\mathbf{1}, \tag{23}$$

$$\mathbf{B}^\alpha \equiv \mathbf{A}\mathbf{S}^\alpha + \mathbf{S}^{\alpha^T}\mathbf{A}. \tag{24}$$

Equations 19 and 20 are solved using a modified Newton-Raphson type algo-rithm. Once $\mathbf{T}^*(\tau)$ and $s^\alpha(\tau)$ are obtained, $\mathbf{F}^p(\tau)$ is obtained by equation 18, $\mathbf{F}^*(\tau)$ is computed using 17b, the crystal stress is calculated using equation 5, the volume averaged macroscopic stress $\bar{\mathbf{T}}$ using equation 1, and the evolution of texture using equations 15 and 16.

SLIP SYSTEM HARDENING RATE

We consider the following form for the single slip hardening rate in equation 14 :

$$h^{(\beta)} = h_o \left\{ 1 - \frac{s^\beta}{s_s} \right\}^a, \tag{25}$$

where h_o, a, and s_s are slip system hardening parameters which are taken to be identical for all slip systems.

Following Asaro and Needleman[1], we take the elements of $q^{\alpha\beta}$ to be equal to 1.0 for systems α and β coplanar and 1.4 for systems α and β non-coplanar.

The hardening parameters for annealed OFHC copper were found by curve-fitting the numerical simulation for uniaxial compression to the experimental data. In the numerical simulations, we took the slip system rate sensitivity m in equa-tion 12 equal to the macroscopic rate sensitivity 0.012 determined from strain rate jump tests in compression at room temperature and $\dot{\gamma}_0$ equal to $0.001 s^{-1}$. The values were estimated to be

$$h_o = 180 \text{ MPa}, \quad s_s = 148 \text{ Mpa}, \quad a = 2.25, \quad s_o = 16 \text{ MPa},$$

where s_0 is the initial slip resistance. The correpondence between simulation of uniaxial compression with the experimental data is shown in Fig. 1.

EXPERIMENTS AND SIMULATIONS

Polycrystalline OFHC copper was deformed in uniaxial compression, uniaxial tension, plane strain compression, planar simple shear, and thin-walled tubular torsion. All experiments were performed at room temperature and an equivalent strain rate of $0.001 s^{-1}$. All copper stock was heat-treated at 800° C in argon for 1 hour. Crystallographic texture was measured by X-ray diffraction to 75° by the Schulz reflection method. Experimental pole figures were processed by using the Preferred Orientation Package from Los Alamos[4].

Simulations were performed assuming an initially random crystallographic tex-ture with a set of 100 crystals. Simulated and experimental stress-strain responses for tension, plane strain compression, and simple shear are shown in Figs. 2, 3, and 4. Simulated and experimental {111}, equal area pole figures for initial unde-formed, compression, tension, plane strain compression, and planar simple shear

are shown in Fig. 5. The marked discrepancy between the simulated and experimental plane strain compression stress-strain curves is attributed to shear bands, which were found to appear between plastic strain levels of -0.21 and -0.52. We see in Fig. 5c that this localization seems to have little influence upon the crystallographic texture developed.

Overall, the constitutive model performs well in predicting both the macroscopic stress-strain response and the evolution of crystallographic texture.

ACKNOWLEDGEMENT

REFERENCES

1. G. I. Taylor, *J. Inst. Metals*, **62**, 307 (1938)
2. R. J. Asaro and A. Needleman, *Acta metall.*, **33**, 923 (1985)
3. L. Anand, *Int. J. Plast.*, **1**, 213 (1985)
4. J. S. Kallend, U. F. Kocks, A. D. Rollett, and H.-R. Wenk, *popLA: the Preferred Orientation Package from Los Alamos*, (August 1989)
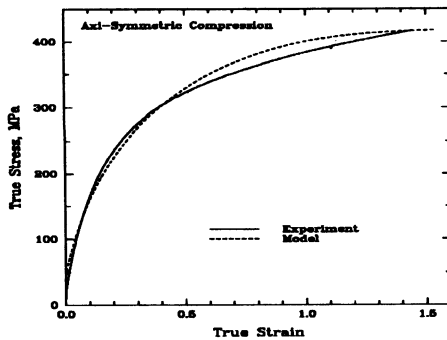
Figure 1: Experimental and simulated response to uniaxial compression.
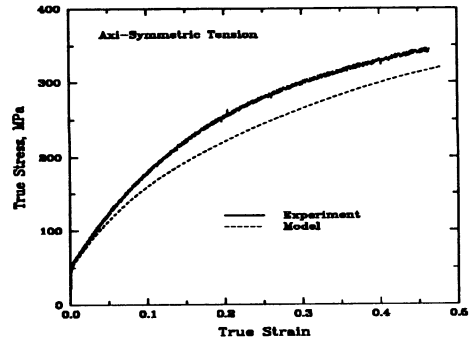

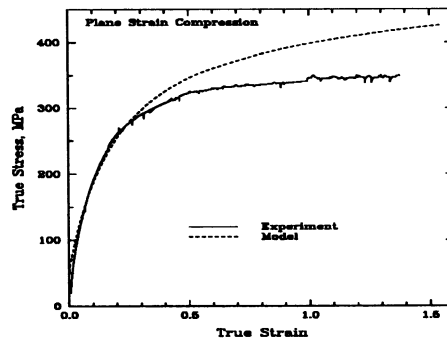Figure 2: Experimental and simulated response to uniaxial tension.

Figure 3: Experimental and simulated response to plane strain compression.
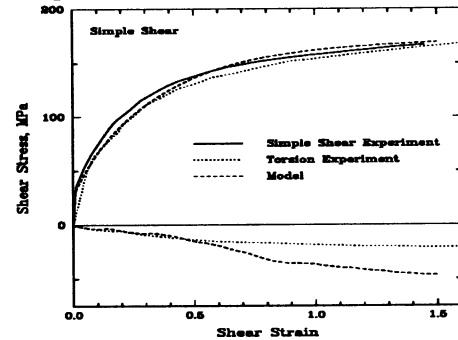

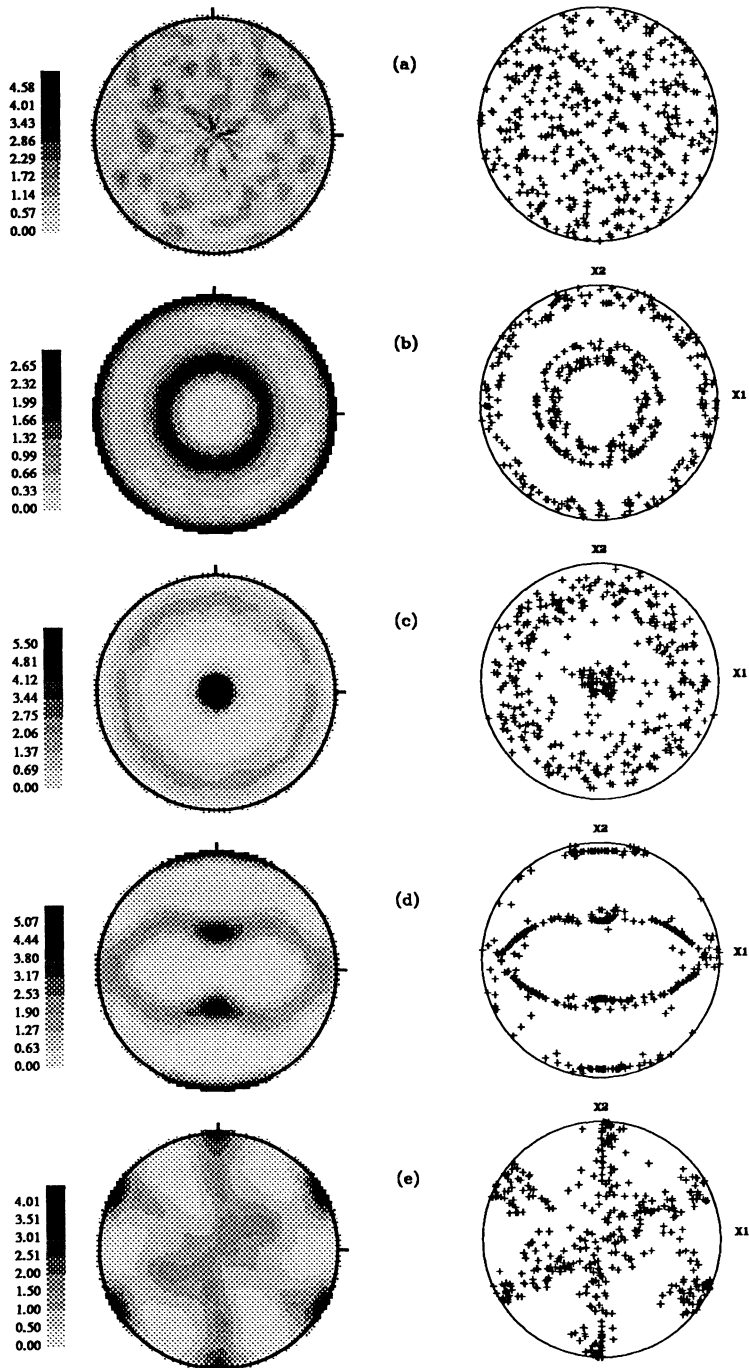Figure 4: Experimental and simulated response to simple shear.

Figure 5: Experimental and Simulated $\{111\}$, equal area pole figures; (a) initial; (b) uniaxial compression, $\epsilon_{33} = -1.53$; (c) uniaxial tension, $\epsilon_{33} = 0.37$; (d) plane strain compression, $\epsilon_{11} = 0, \epsilon_{33} = -1.54$; (e) planar simple shear, $\gamma_{12} = -1.40$.